Title: Label-free pharmacological profiling based on dynamic mass redistribution for characterization and authentication of hazardous natural products

Authors: Hui-Peng Song, Hong Wang, Xiaoai Zhao, Ling He, Huailing Zhong, Si-Qi Wu, Ping Li, Hua Yang

PII: S0304-3894(17)30191-7
DOI: http://dx.doi.org/doi:10.1016/j.jhazmat.2017.03.025
Reference: HAZMAT 18441

To appear in: *Journal of Hazardous Materials*

Received date: 4-12-2016
Revised date: 10-3-2017
Accepted date: 11-3-2017

Please cite this article as: Hui-Peng Song, Hong Wang, Xiaoai Zhao, Ling He, Huailing Zhong, Si-Qi Wu, Ping Li, Hua Yang, Label-free pharmacological profiling based on dynamic mass redistribution for characterization and authentication of hazardous natural products, Journal of Hazardous Materials http://dx.doi.org/10.1016/j.jhazmat.2017.03.025

Label-free pharmacological profiling based on dynamic mass redistribution for characterization and authentication of hazardous natural products

Hui-Peng Song[a,1], Hong Wang[a,1], Xiaoai Zhao[b], Ling He[a,c], Huailing Zhong[d], Si-Qi Wu[a], Ping Li[a,*], Hua Yang[a,*]

[a] State Key Laboratory of Natural Medicines, China Pharmaceutical University, Nanjing 210009, China

[b] Department of Genetics, Stanford University, Stanford, CA 94305 USA

[c] Department of Pharmacology, China Pharmaceutical University, Nanjing 210009, China

[d] U-Pharm Laboratories LLC, 239 New Rd, Suite A-107, Parsippany, NJ 07054 USA

* Corresponding authors at: China Pharmaceutical University, No. 24, Tongjia Lane, Nanjing, China.

[1] These authors contributed equally to this work.

Tel.: +86 25 8327 1379; fax: +86 25 8327 1379.

E-mail addresses: liping2004@126.com (P. Li), 104yang104@163.com (H. Yang).

Graphical abstract

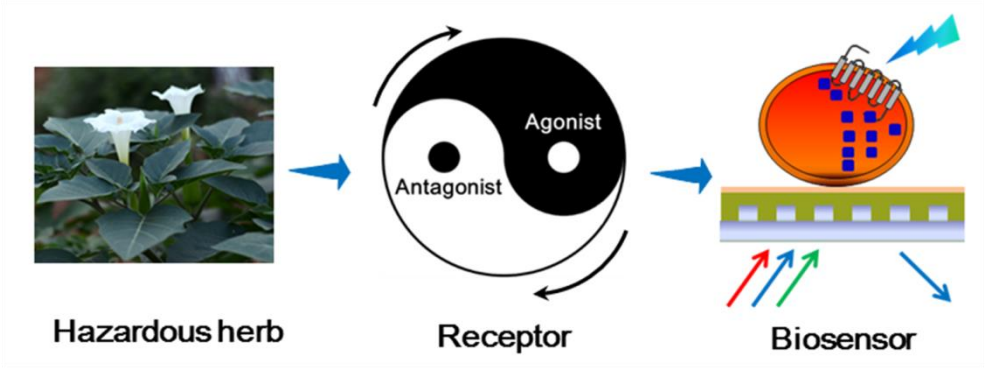

Highlights

1. Dynamic mass distribution (DMR) profiling was proposed to characterize toxic herbs.
2. Qualitative DMR profiling has obvious advantages over the classic method.
3. Quantitative DMR profiling was powerful in discovery of toxic marker compounds.
4. The proposed method is high-throughput, cost-saving and easily operated.
5. DMR profiling is universal for discovery of most receptor-targeted toxicants.

Abstract:

Natural products are becoming increasingly popular in multiple fields involving medicines, foods and beverages. However, due to the frequent occurrence of poisoning incidents, their toxicity and safety have caused a serious concern. Here we report a method of biosensor-based two-phase pharmacological profiling (BTPP) for discovery, monitor and control of receptor-targeted natural products. BTPP uses a resonant waveguide grating biosensor for label-free and non-invasive detection of intracellular dynamic mass distribution (DMR), a phenomenon caused by protein relocalization after receptors receiving stimulation from toxicants. The method can not only facilitate the identification of hazardous materials but also quantify their bioactivity by EC_{50}. As a proof of concept, the method was successfully applied to recognize *Daturae Flos* (*DF*), an herb that can antagonize muscarinic acetylcholine M_2 receptor and further cause poisoning, from other easily confused species. BTPP combined with high performance liquid chromatography revealed that scopolamine and hyoscyamine in *DF* are the key marker compounds. Moreover, the method accurately picked out 2 M_2 receptor antagonists from 25 natural compounds, displaying its potential in high-throughput screening. This study provides a systematic illustration about the establishment, applicability and advantages of BTPP, which contributes to the safety assessment of natural products in related fields.

Keywords: dynamic mass redistribution; hazardous herbs; receptor; pharmacological profiling

1. Introduction

Natural products (NPs) have been an indispensable part of human life: almost 50% of drugs in use today directly or indirectly come from NPs [1], many natural additives such as vitamin C are necessities in daily life [2], and herbal medicines play an important role in developing countries for disease treatment [3,4]. As NPs penetrate into various fields, their safety issues, especially the frequent poisoning accidents caused by misuse and confusion of herbs, have aroused increasing attention [5]. Actually, many herbs with impressive therapeutic effects are demonstrated to be toxic [6]. For instance, *Daturae Flos* (*DF*) is a potent herbal medicine for anti-asthma, but it could also be poisonous by antagonizing muscarinic acetylcholine M_2 receptor. Due to the similar appearance of dried herbs or homonyms-confusion in local dialect [5], *DF* is easily misused with other non-toxic ones such as *Rhododendri Mollis Flos* and *Lonicera Japonica Flos* [7,8]. Current methods for herb authentication mainly include morphology [9], chemotaxonomy [10], microscopy [11], chromatography [12] and DNA barcoding [13]. However, all the methods are based on the physical or chemical characteristics rather than the intrinsic toxicity [14]. Recently Qin *et al.* proposed that mice, rats, guinea pigs and pigeons could be used as models to evaluate the toxicity of herbs [15]. Nevertheless, this approach is easily confined by the high cost and low throughput of animal experiments. As herb-derived natural products are becoming more and more popular worldwide [16,17], establishment of efficient and high-throughput methods for quality control of herbs has been an urgent and important task.

Membrane receptors are recognized as critical toxicological targets [18]. When a receptor is stimulated, the downstream events like cAMP alteration, protein trafficking and kinase phosphorylation will be triggered [19]. Traditional methods for receptor assays mainly rely on the detection of some single event, and have been demonstrated to be effective in many studies [20]. However, there are several defects that have limited their application: (1) most events have to be tagged with fluorescent labels leading to the impact on normal cellular physiology [21]; (2) traditional methods are usually invasive and require cell rupturing [22]; (3) any single event could not fully reflect the whole receptor cascade [23]. To overcome the above limitations, an emerging technology of resonant waveguide grating (RWG) biosensors was proposed [24]. Its detection principle is to convert dynamic mass redistribution (DMR), a phenomenon of intracellular protein delocalization after the receptor receiving stimulation, into a quantifiable optical signal (Fig. 1A) [25,26]. This method facilitates direct and non-invasive monitoring of whole-cell responses, and thus there is no need to label an event or rupture the cells. Moreover, the kinetic DMR profiling can give abundant real-time information about intracellular change, which is helpful for the investigation of potential biochemical mechanisms [27,28]. Because of the above features, RWG biosensors have become an important tool for receptor biology, and their application fields are continuously expanding [29].

In this study, a novel method of biosensor-based two-phase pharmacological profiling (BTPP) was established to characterize and authenticate receptor-targeted hazardous natural products. Its design concept is inspired from Yin-Yang theory of the

traditional medical system (Fig. 1B), which is now a part of complementary and alternative medicines. There are three important points in the theory: (1) Yin and Yang are two opposite aspects for one objective. (2) Yin and Yang are incompatible with each other but in a dynamic balance. (3) The phenotype of an objective is the internal integration of Yin and Yang. As for receptors, antagonists and agonists are corresponding to Yin and Yang, respectively. The final pharmacological phenotype is based on the competition between antagonists and agonists for receptors. Guided by this theory, the BTPP method is designed as follows. In phase I, the potential toxicant directly acts on the receptor, of which the phenotype is detected by a RWG biosensor. In phase II, a known probe molecule with an opposite effect is added to cause Yin-Yang interaction, and the generated phenotype could quantitatively reflect the competitiveness of the toxicant for receptors. Taking *Daturae Flos* (*DF*) as an illustrative case, we demonstrated the effectiveness and reliability of BTPP in recognizing the poisonous herb from other non-toxic ones. Compared with the classic method of microscopic identification, BTPP showed obvious advantages in convenience, throughput and accuracy. The proposed method can be used as a simple but efficient alternative for characterization of receptor-targeted toxicants.

2. Experimental

2.1 Materials and reagents

Scopolamine and atropine were purchased from Aladin Chemical Co., Ltd (St. Louis, Mo, USA). Acetylcholine chlorine and dimethyl sulfoxide (DMSO) were obtained

from Sigma (St. Louis, MO, USA). The 25 reference compounds for activity screening were acquired from Chengdu Must Bio-technology Co., Ltd (Chengdu, China). Acetonitrile (HPLC grade) were purchased from Merck (Darmstadt, Germany). Ultra-pure water was prepared with a Milli-Q water purification system (Millipore, Bedford, MA, USA). Potassium dihydrogen phosphate (KH_2PO_4), sodium heptane-1-sulfonate ($C_7H_{15}O_3SNa$) and phosphoric acid were of analytical purity and purchased from Shanghai Lingfeng Chemistry Reagents Co., Ltd.

2.2 Extraction of Daturae Flos (*DF*)

A total of 20 batches of *DF* were collected from various areas in China. They were powdered by a grinder and sieved to a homogeneous size. One gram of powder was accurately weighed and immersed in 10 ml of 2 M hydrochloric acid. After a 30-min ultra-sonication, the extract was alkalized with ammonia solution (pH=9) and extracted with 10 ml of trichloromethane for four times. Trichloromethane layers were combined and evaporated to dryness. The residues were dissolved with Hank's balanced salt solution (HBSS) and transferred to a 5-ml volumetric flask. The solutions were further diluted with HBSS to volume, and then centrifuged at 13, 000 rpm for 10 min. The supernatants were stored at 4 °C for use [30].

2.3 Conditions of chromatographic separation

Chromatographic analysis was performed on an Agilent 1100 series LC system (Agilent Technologies, USA) equipped with a binary pump, an online degasser, an

auto sampler, a thermostatically controlled column compartment and a diode array detector. The separation of *DF* was achieved on an Agilent C_{18} column at room temperature (250 mm × 4.6 mm, 5 μm, Agilent Technologies, Santa Clara, CA, USA). The mobile phase consisted of 0.05 mol/L KH_2PO_4 aqueous solution containing 0.0025 mol/L $C_7H_{15}O_3SNa$ (A) and acetonitrile (B). The pH of mobile phase A was adjusted to 5 with phosphoric acid. The elution program is as flows: 0-13 min, 16-16% (B); 13-20 min, 16-18% (B); 20-28 min, 18-18% (B); 28-30 min, 18-20% (B); 30-42 min, 20-20%; 42-60 min, 20-25%. The flow rate was 1.0 mL/min. The wavelength was set at 215 nm.

2.4 Cell culture

Three cell lines including H9c2 cardiomyocytes, human aortal vascular endothelial cells (HAVEC) and CHO-M_2 were cultured in Dulbecco's modified Eagle's medium (DMEM), RPMI-1640 and HyClone Ham's F-12 Nutrient Mixture, respectively. All the mediums were supplemented with 10% fetal bovine serum (FBS), 80 U/mL penicillin and 0.08 mg/mL streptomycin. CHO-M_2 is Chinese hamster ovary (CHO) cells, in which the muscarinic acetylcholine M_2 receptor was stably expressed. To maintain the cell's states, 0.4 mg/ml geneticin and 0.25 mg/mL zeocin were added to its medium. All the cells were grown at 37 °C under a humidified atmosphere with 5% (v/v) CO_2.

2.5 Assay of dynamic mass redistribution (DMR) in cell

The dynamic mass redistribution (DMR) was measured by an optical biosensor (Epic system, Corning) [31]. About 25, 000 cells were seeded in each well of the Epic 384-well cell assay plates (Corning 5040) and cultured for 14 hours. After that, the medium was removed, and 20 μL of HBSS was added into each well. The microplate was put into Epic reading system for signal balancing. After 1 hour, a new reading program was started and the signal baseline was normalized to zero. The baseline was recorded for 2 min, and then the reader was paused. Subsequently, 10 μL of the test solution was transferred into each microplate well. The program continued to read for 1 hour, and the recorded signal was the DMR profiling of phase I. In the following phase II, 10 μL of acetyl choline (16 μM) was added to the measure system with a similar operation, and another 1-hour DMR profiling was obtained. All procedures were carried out with four replicates. Statistical analyses were performed with GraphPad Prism version 6.02 software (GraphPad Software Incorporated).

2.6 Fingerprint-efficacy correlation analysis

The HPLC files with the suffix of "AIA" were imported into professional software named *similarity evaluation system for chromatographic fingerprint of TCM* [32]. After the procedure of multi-point correction, 7 common peaks were recognized by automatic matching of the chromatographic fingerprints of 20 batches of *DF*. Based on the 7 common peaks, a total of 127 possible combinations were generated according to the algorithm of permutation and combination. The sum of peak areas in each combination was computed to form a dataset. The EC_{50} values of 20 batches of

DF constituted the 128th dataset. Pearson correlation coefficients between the 127 datasets of combinations and the 128th dataset of bioactivity were calculated by IBM SPSS statistics software (version 19.0, SPSS Inc., USA) [33]. To further analyze the relationship between correlation coefficients and combinations, Hierarchical cluster analysis, which can group combinations based on the similarity of correlation coefficients, was conducted using PermutMatrixEN software [34]. To make the complex data visual, heatmap and dendrogram were adopted.

2.7 Molecular docking and pharmacophore modeling

To explore the probable binding interactions of the antagonists with M_2 receptor, AutoDock (version 4.2) was performed according to the standard protocol [35]. The X-ray crystal structure of M_2 receptor was downloaded from Protein Data Bank (http://www.rcsb.org/pdb, PDB ID: 4MQS), which is pretreated by adding polar hydrogens and Kollman charges. The structures of compounds including scopolamine, hyoscyamine, chelerythrine and sanguinarine were constructed in ChemBioDraw Ultra 12.0, and their energies were minimized by ChemBio3D Ultra 12.0. In AutoGrid process, the whole protein of M_2 receptor was covered by a grid box to generate a pre-calculated grid map. A widely accepted method of Lamarckian genetic algorithm was adopted to conduct AutoDock. The docking runs are set as 100, and the other parameters are default. Among the generated simulations, the most stable conformation with the lowest binding energy was used to elucidate the binding modes between antagonists and receptor.

The pharmacophore modeling was conducted using the Hip-Hop of Discovery Studio 2.0 (Accelrys, San Diego, CA, USA) [36]. Based on the structural similarities, the four bioactive compounds were divided into two groups, namely, group 1 (scopolamine and hyoscyamine) and group 2 (chelerythrine and sanguinarine). The common pharmacophore features of above two groups were mapped, respectively. The parameters were as follows: hydrogen bond acceptor, hydrogen bond donor, hydrophobic, pos ionizable and ring aromatic were selected as features; conformation generation, best; maximum conformation, 200; energy threshold, 10 kcal/mol; maximum pharmacophores, 10; minimum interfeature distance, 2.97 Å. The other parameters were set as default. The generated pharmacophore model with the highest score was applied for analysis.

3. Results and discussion

3.1 Biosensor-based two-phase pharmacological profiling (BTPP)

Screening for a suitable cell that can generate DMR signal is the prerequisite for establishment of BTPP. An ideal cell should satisfy the following two conditions: (1) there are abundant target receptors on the cell membrane; (2) the interaction of the target receptor and its agonist could cause DMR that is detectable by the RWG biosensor. Three cell lines including H9c2 cardiomyocyte, HAVEC and CHO-M_2 were tested. Fortunately, CHO-M_2 produced an obvious dose-dependent response when it was activated by the agonist acetylcholine (Fig. 2C). Based on this cell, BTPP with two-phase phenotypes were designed for characterization of *Daturae Flos* (*DF*).

In phase I, *DF* extract directly acts on the CHO-M_2 cell, for which the DMR signal is recorded by the biosensor. The signal has 3 possible phenotypes including signal rise (1), no change (0) and signal drop (-1) as shown in Fig. S1A. In phase II, acetylcholine is added to the reaction system to compete with *DF* extract for the receptors. Due to the antagonism of *DF* extract, the DMR signal caused by acetylcholine is inhibited. When the concentration of *DF* extract is high enough, the DMR signal will be completely suppressed. However, the extracts of other non-toxic herbs cannot antagonize M_2 receptor, and thus they will not impact the signal rise (1) in Phase II. Because there is 3 possible phenotypes in each phase, BTPP with two phases has 9 possible combinations (3×3) (Fig. S1B). Theoretically, *DF* is specifically corresponding to one of the 9 phenotypes, and other herbs lies within the scope of the other 8 phenotypes. To verify the feasibility of above idea, we collected 20 batches of *DF* from different areas in China and tested their phenotypes according to the procedure described in Section 2.5. As shown in Fig. S2, all the *DF* extracts exhibited the same phenotype of (1, 0), suggesting that it was a common characteristic for *DF*. The 7 easily confused herbs were also assayed with the phenotypes of (1, 1) or (0, 1) as shown in Fig. 3. By comparing the results, *DF* was easily distinguished from the other herbs, indicating that BTPP is feasible for recognition of a receptor-targeted substance.

3.2 Comparison of BTPP with microscopic authentication

It is necessary to compare the proposed approach with the classical one. Therefore,

microscopic authentication, a method that is a widely accepted by multiple pharmacopeias, was conducted as contrast. The principle of microscopic authentication is to analyze the cell, structure and internal characteristics of herbs through a microscope. As shown in Fig. S3, pollen grain (A), non-glandular hair (B), vessel (C), cluster (D), prism (E) and sand crystal (F) could be found in the *DF* powder, of which the features are consistent with the records in pharmacopeias. However, when these features of *DF* were compared with those of other herbs, the distinctions were not so obvious. Table S1 shows the comparison of pollen grain and non-glandular hair of the eight herbs. The main characteristics of *DF* are as the followings: (1) the surface of pollen grain forms striped sculpture; (2) the non-glandular hair contains multiple cells, of which the wall is decorated with warty dots. Compared with the digital presentation such as (1, 0) of BTPP method, these delicate characteristics obtained by microscope are not easy to observe. Its accuracy is largely dependent on the knowledge and experience of an operator, which can cause misidentifications due to the subjective bias. Moreover, microscopic authentication has only one channel, whereas BTPP is high-throughput with 384 channels. That means the efficiency of the latter is two orders of magnitude more than that of the former. Although BTPP shows obvious advantages in multiple aspects, it does not indicate that BTPP could replace microscopic authentication because they are based on different principles. It is expected that BTPP and microscopic authentication could work cooperatively to recognize hazardous herbs and avoid poisoning incidents.

3.3 Prediction of marker compounds in DF by fingerprint-efficacy correlation analysis

Herbs are multi-component complex systems. Discovery of marker compounds that are responsible for the toxicity is the key for understanding hazardous herbs [37]. Fingerprint-efficacy correlation analysis is an emerging method for prediction of marker compounds related to the bioactivity of herbs [38]. This method requires multiple batches of samples, for which the bioactivity values and chromatographic fingerprints could be correlated. In this case, a total of 20 batches of *DF* were collected. Their fingerprints were acquired by an optimized ion-pairs HPLC method as shown in Fig. 4. Since the phenotype in phase II directly reflects the antagonism effect of *DF* on M_2 receptor, we tried to quantify this phenotype to obtain the EC_{50}. The DMR signals for different concentrations of *DF* are shown in Fig. 5A. The max DMR values show an obvious concentration-dependent manner (Fig. 5B), and thus these data are inputted into software for simulation of the bioactivity curves. Finally, the EC_{50} values of 20 batches of *DF* were calculated as summarized in Table 1. Interestingly, we found that *DF* from southern China usually showed stronger antagonistic activity at M_2 receptor. This may be due to the warm climate, plenty rainfall and abundant sunshine in this region, which are beneficial to the growth of medicinal plants and the accumulation of bioactive components.

Pearson correlation coefficient and hierarchical cluster analysis were adopted to establish the fingerprint-efficacy relationship. Ideal marker compounds are usually the common components of herbs in different areas. Here, a total of 7 common peaks

were recognized in the fingerprints (Fig. 4). Since the number of marker compounds was unknown, we hypothesized that it might be 1, 2, 3, 4, 5, 6 or 7. Correspondingly, the number of peak combinations is 7, 35, 21, 21, 35, 7 or 1 based on the algorithm of permutation and combination. The correlation coefficients between the above peak combinations and EC_{50} were calculated by person analysis and ranked by Hierarchical analysis. The results are displayed with heat maps, in which red indicates high correlation and green represents low relativity. As shown in Fig. 6A, the correlation coefficients of 7 single peaks were ranked as: 3 > 2 > 1 > 7 > 6 > 4 > 5. By comparing the coefficients of multi-peak combinations (Fig. 6B-E), it could be observed that the combinations containing peak 2 or peak 3 were in the top. Correspondingly, the combinations without peak 2 or peak 3 were at the bottom. When peak 2 and peak 3 coexist in the one combination, the correlation coefficient was higher than that of the combination containing only peak 2 or peak 3 (Fig. 6F). All the results indicated that the two peaks might be the potential marker compounds of *DF*.

3.4 Qualitative and quantitative analysis of peak 2 and peak 3

Structural identification of the potential marker compounds was conducted by high-resolution time-of-flight (TOF) mass. The positive quasi-molecular ions of peak 2 and peak 3 were at m/z 304.1548 and 290.1753, respectively. Based on the accurate molecular weight, the corresponding molecular formulas, namely, $C_{17}H_{21}NO_4$ and $C_{17}H_{23}NO_3$, were rapidly found from the compound library. By comparing mass data, retention time and UV absorption with those of reference compounds, peak 2 and

peak 3 were identified as scopolamine and hyoscyamine, respectively. Furthermore, we established the quantitative methods of the two compounds including quantitative equations, linear ranges, limits of detection (LOD) and limits of quantification (LOQ) as shown in the following Fig. 7. The contents of scopolamine and hyoscyamine in 20 batches of *DF* were then analyzed and summarized in Table 1.

3.5 Bioactivity validation of the discovered marker compounds

To verify the potential marker compounds, quantitative BTPP experiments were conducted. As shown in Fig. S4, either scopolamine or hyoscyamine antagonized the acetylcholine-induced DMR signal with a concentration-dependent manner, which is highly similar with that of *DF* extract (Fig. 5). The EC_{50} values of scopolamine and hyoscyamine were 0.27 μM (81.90 ng/mL) and 0.16 μM (46.30 ng/mL), respectively, indicating that they are potent M_2 receptor antagonists.

To evaluate the bioactivity contribution of marker compounds, we prepared a mixture containing scopolamine and hyoscyamine, of which the contents were the same as those in *DF*. By comparing the bioactivity of the mixture and *DF* extract, the importance of scopolamine and hyoscyamine in *DF* could be assessed. Among the 20 batches of *DF*, the No. 5 possessed the strongest effect (EC_{50} = 5.86 μg/mL, Table 1), and thus it was chosen to illustrate this case. As shown in Fig. 8, the bioactivity curves of the prepared mixture (red) and *DF* extract (blue) are alike. The EC_{50} of the former was 6.29 μg/mL, close to that of the latter (5.86 μg/mL), suggesting that hyoscyamine and scopolamine were the bioactive equivalent components of *DF*. To further explore

the contribution of each component, hyoscyamine and scopolamine were tested individually. It could be seen the curve of hyoscyamine (green) or scopolamine (black) is significantly rightward shifted compared to that of *DF* (Fig. 8). Their EC_{50} values (43.59 μg/mL and 42.46 μg/mL) were also an order of magnitude higher than that of *DF* extract (5.86 μg/mL), indicating that neither of them could represent *DF*. In summary, scopolamine and hyoscyamine were the key active components of *DF*, and they should be simultaneously used as the marker compounds for quality control.

3.6 Screening for hazardous natural products by BTPP

To expand the application scope, BTPP was used to discover potential M_2 receptor antagonists from 25 natural products that were widely distributed in the environment. To ensure the reliability of obtained phenotypes, the 25 natural compounds at three gradient concentrations of 6.25, 25 and 100 μM were assayed. The results are shown in Table 2. Based on the previous analysis, if a compound can antagonize M_2 receptor, its phenotype in phase II should be "0". According this criterion, chelerythrine (4) and sanguinarine (16) were preliminarily regarded as the M_2 receptor antagonists. Followed by the quantitative BTPP experiments, their EC_{50} values were determined as 14.29 and 5.65 μM, respectively. To evaluate the toxicities of above two compounds, acute toxicity tests in mice were conducted. The detailed procedures and data are shown in Section 1.6 of Supplementary Material. Finally, the intraperitoneal median lethal dose (LD_{50}) values of chelerythrine and sanguinarine were determined to be 23.8 and 28.6 mg/kg, respectively. The results implies that the herbs such as

Chelidonium majus, *Toddalia asiatica (L.) Lam.* and *Corydalis edulis Maxim.*, of which the main component is chelerythrine or sanguinarine, might be potentially harmful. High alertness must be kept when these herbs are used as health products, teas or medicines.

3.7 Mechanism exploration by pharmacophore modeling and molecular docking

To explore the mechanisms of M_2 receptor antagonists, pharmacophore modeling and molecular docking were conducted. Pharmacophore modeling is a ligand-based approach to extract the common structural features that are responsible for the bioactivity, whereas molecular docking is a receptor-based method to predict the preferred binding orientation of one compound to a receptor. By integrating the two methods, the potential action mechanisms of M_2 receptor antagonists could be elucidated from the perspectives of ligand and receptor.

In this study, four natural products including scopolamine, hyoscyamine, chelerythrine and sanguinarine were identified as M_2 receptor antagonists by BTPP. Their EC_{50} values, chemical structures, pharmacophore features and docking simulations are shown in Table 3. Interestingly, the four compounds could be divided into two types according to the structural similarities: scopolamine and hyoscyamine could be seen as the ester of tropane-derived amino alcohol and aromatic acid (type 1); chelerythrine and sanguinarine share a common nucleus with 21 atoms arranged in five rings (type 2). The pharmacophore features of type 1 are composed of one hydrogen bond acceptor (green), one aromatic ring (brown), hydrogen bond donor

(magenta) and one cation (red); the pharmacophore features of type 2 consist of one aromatic ring (brown), two hydrophobic centers (cyan) and two hydrogen bond acceptors (green). It could be observed that the differences between the two pharmacophores are obvious, implying that their action mechanisms on M_2 receptor are distinguished. It is widely known that the M_2 receptor is a typical seven-transmembrane protein as marked by TM 1-7 in the last column of Table 3. According to the reported literatures [39,40], acetylcholine actives the muscarinic receptor by binding to the cavity formed by TM3, TM5, TM6 and TM7. Coincidentally, scopolamine and hyoscyamine also bound in this position, indicating that they compete with Ach for this site to exert the powerful antagonism effects. However, chelerythrine or sanguinarine interacted with the channel among TM2, TM3, TM6 and TM7, which was not completely consistent with the binding site of Ach. The above results might explain why the EC_{50} values of chelerythrine (14.29 μM) and sanguinarine (5.65 μM) are higher than those of scopolamine (0.27 μM) and hyoscyamine (0.16 μM).

4. Conclusions

This study reports a method of biosensor-based two-phase pharmacological profiling (BTPP) for characterization of receptor-targeted hazardous natural products. By comparing with the classic method, the advantages of BTPP include the followings: (1) its throughput was two magnitudes higher than that of microscopic authentication; (2) it is less dependent on the accumulated knowledge of the operator; (3) the digitized

result is easily analyzed and can avoid misjudgments. Besides, the developed quantitative BTPP shows good compatibility with fingerprint-efficacy correlation, which could be coordinately applied for identification of marker compounds in herbs. Notably, BTPP is suitable for not only the poisonous natural products but also other receptor-targeted toxicants such as pesticides and dioxins. The high-throughput BTPP method is expected to be a practical tool for monitor and control of hazardous substances in multiple fields such as medicine, food and environment.

Acknowledgements

This work was supported by the Foundation for Innovative Research Groups of the National Natural Science Foundation of China (Grant No. 81421005), and a Project Funded by the Priority Academic Program Development of Jiangsu Higher Education Institutions. The authors thank Dr. Mei Tian, Dr. Geng-Yu Lu and Miss Yue-Hua Chen of China Pharmaceutical University for providing us the pictures of plants.

References

1 D.J. Newman, G.M. Cragg, Natural products as sources of new drugs from 1981 to 2014, J Nat. Prod. 79 (2016) 629-661.

2 H.P. Song, S.Q. Wu, L.W. Qi, F. Long, L.F. Jiang, K. Liu, H. Zeng, Z.M. Xu, P. Li, H. Yang, A strategy for screening active lead compounds and functional compound combinations from herbal medicines based on pharmacophore filtering and knockout/knockin chromatography, J. Chromatogr. A 1456 (2016) 176-186.

3 S. Hasani-Ranjbar, N. Nayebi, B. Larijani, M. Abdollahi, A systematic review of the efficacy and safety of herbal medicines used in the treatment of obesity, World J. Gastroenterol. 15 (2009) 3073-3085.

4 H.P. Song, H. Zhang, Y. Fu, H.Y. Mo, M. Zhang, J. Chen, P. Li, Screening for selective inhibitors of xanthine oxidase from Flos Chrysanthemum usingultrafiltration LC-MS combined with enzyme channel blocking, J. Chromatogr. B Analyt. Technol. Biomed. Life Sci. 961 (2014) 56-61.

5 Z. Zhao, Y. Hu, Z. Liang, J.P. Yuen, Z. Jiang, K.S. Leung, Authentication is fundamental for standardization of Chinese medicines, Planta Medica 72 (2006) 865-874.

6 C. Chu, L. Xia, L.P. Bai, Q. Li, H.B. Chen, Z.Z. Zhao, Authentication of the 31 species of toxic and potent Chinese materia medica by light microscopy, part 3: Two species of T/PCMM from flowers and their common adulterants, Microsc. Res. Tech. 72 (2009) 454-463.

7 K.Y. Ng, C.L. Cheng, H.X. Xu, Safety issues of Chinese medicine: a review of

intoxication cases in Hong Kong, Chin. Herb. Med. 1 (2009) 29-39.

8 X.L. Xu, Y. Shang, J.G. Jiang, Plant species forbidden in health food and their toxic constituents, toxicology and detoxification, Food Funct. 7 (2016) 643-664.

9 M. Zafar, M.A. Khan, M. Ahmad, S. Sultan, R. Qureshi, R.B. Tareen, Authentication of misidentified crude herbal drugs marketed in Pakistan, J. Med. Plants Res. 4 (2010) 1584-1593.

10 M. Ahmad, M.A. Khan, A. Hasan, M. Zafar, S. Sultana, Chemotaxonomic standardization of herbal drugs milk thistle and globe thistle, Asian J. Chem. 20 (2008) 4443-4459.

11 Z.Z. Zhao, Y.N. Hu, Y.W. Wong, W.C. Gigi Wong, Application of microscopy in authentication of Chinese patent medicine-Bo Ying compound, Microsc. Res. Tech. 67 (2005) 305-311.

12 P.S. Xie, Y.Z. Yan, B.L. Guo, C.W. Lam, S.H. Chui, Q.X. Yu, Chemical pattern-aided classification to simplify the intricacy of morphological taxonomy of Epimedium species using chromatographic fingerprinting, J. Pharm. Biomed. Anal. 52 (2010) 452-460.

13 T. Gao, S.L. Chen, Authentication of the medicinal plants in Fabaceae by DNA barcoding technique, Planta Medica 75 (2009) 417-417.

14 Kunle, O. Folashadel, Egharevba, H. Omoregie, Ahmadu, P. Ochogu, Standardization of herbal medicines-A review, Int. J. Biodivers. Conserv. 4 (2012) 101-112.

15 Y. Qin, J.B. Wang, Y.L. Zhao, L.M. Shan, B.C. Li, F. Fang, C. Jin, X.H. Xiao,

Establishment of a bioassay for the toxicity evaluation and quality control of Aconitum herbs, J. Hazard. Mater. 199 (2012) 350-357.

16 H.P. Song, J. Chen, J.Y. Hong, H.P. Hao, L.W. Qi, J. Lu, Y. Fu, B. Wu, H. Yang, P. Li, A strategy for screening of high-quality enzyme inhibitors from herbal medicines based on ultrafiltration LC-MS and in silico molecular docking, Chem. Commun. 51 (2015) 1494-1497.

17 H.P. Song, S.Q. Wu, H.P. Hao, J. Chen, J. Lu, X.J. Xu, P. Li, H. Yang, A chemical family-based strategy for uncovering hidden bioactive molecules and multicomponent interactions in herbal medicines, Sci. Rep. 6 (2016) 23840.

18 M. Pohanka, Alpha7 nicotinic acetylcholine receptor is a target in pharmacology and toxicology, Int. J. Mol. Sci. 13 (2012) 2219-2238.

19 Y. Fang, Label-free receptor assays, Drug Discov. Today Technol. 7 (2011) e5-e11.

20 C.W. Scott, M.F. Peters, Label-free whole-cell assays: expanding the scope of GPCR screening, Drug Discov. Today 15 (2010) 704-716.

21 P.H. Lee, A. Gao, C. Van Staden, J. Ly, J. Salon, A. Xu, Y. Fang, R. Verkleeren, Evaluation of dynamic mass redistribution technology for pharmacological studies of recombinant and endogenously expressed G protein-coupled receptors, Assay Drug Dev. Technol. 6 (2008) 83-94.

22 D. Gabriel, M. Vernier, M.J. Pfeifer, B. Dasen, L. Tenaillon, R. Bouhelal, High throughput screening technologies for direct cyclic AMP measurement, Assay Drug Dev. Technol. 1 (2003) 291-303.

23 M.J. Bround, R. Wambolt, D.S. Luciani, J.E. Kulpa, B. Rodrigues, R.W.

Brownsey, M.F. Allard, J.D. Johnson, Cardiomyocyte ATP Production, Metabolic Flexibility, and Survival Require Calcium Flux through Cardiac Ryanodine Receptors in Vivo, J. Biol. Chem. 288 (2013) 18975-18986.

24 Y. Fang, A.M. Ferrie, N.H. Fontaine, P.K. Yuen, Characteristics of Dynamic Mass Redistribution of Epidermal Growth Factor Receptor Signaling in Living Cells Measured with Label-Free Optical Biosensors, Anal. Chem. 77 (2005) 5720-5725.

25 R. Schröder, J. Schmidt, S. Blättermann, L. Peters, N. Janssen, M. Grundmann, W. Seemann, D. Kaufel, N. Merten, C. Drewke, J. Gomeza, G. Milligan, K. Mohr, E. Kostenis, Applying label-free dynamic mass redistribution technology to frame signaling of G protein-coupled receptors noninvasively in living cells, Nat. Protoc. 6 (2011) 1748-1760.

26 R. Schröder, N. Janssen, J. Schmidt, A. Kebig, N. Merten, S. Hennen, S. Blättermann, S. Zahn, J. Wenzel, N.J. Smith, J. Gomeza, C. Drewke, K. Mohr, E. Kostenis, Deconvolution of complex G protein-coupled receptor signaling in live cells using dynamic mass redistribution measurements, Nat. Biotechnol. 28 (2012) 943-949.

27 A. Bock, B. Chirinda, F. Krebs, R. Messerer, J. Batz, M. Muth, C. Dallanoce, D. Klingenthal, C. Hoffmann, A.M. De, U. Holzgrabe, E. Kostenis, K. Mohr, Dynamic ligand binding dictates partial agonism at a G protein-coupled receptor, Nat. Chem. Biol. 10 (2014) 18-20.

28 S. Hennen, H. Wang, L. Peters, N. Merten, K. Simon, A. Spinrath, S. Blattermann, R. Schrage, R. Schroder, D. Schulz, A. Pfeifer, K. Mohr, M. Gillard, Q.R. Lu, J.

Gomeza, E. Kostenis, Decoding signaling and function of the orphan G protein–coupled receptor GPR17 with a small-molecule agonist, Sci. Signal. 6 (2013) ra93.

29 M.R. Fleming, S.M. Shamah, L.K. Kaczmarek, Use of label-free optical biosensors to detect modulation of potassium channels by G-protein coupled receptors, J. Vis. Exp. 10 (2014) e51307.

30 China Pharmacopeia Committee, Pharmacopoeia of the People's Republic of Chian, China Medical Science Press 1 (2015) 267-267.

31 X.L. Zhang, H.Y. Deng, Y.S. Xiao, X.Y. Xue, A.M. Ferrie, E. Tran, X.M. Liang, Y. Fang, Label-free cell phenotypic profiling identifies pharmacologically active compounds in two Traditional Chinese Medicinal plants, RSC. Adv. 4 (2014) 26368-26377.

32 W.J. Kong, J.B. Wang, Q.C. Zang, X.Y. Xing, Y.L. Zhao, W. Liu, J. Cheng, Z.L. Li, X.H. Xiao, Fingerprint-efficacy study of artificial Calculus bovis in quality control of Chinese materia medica, Food Chem. 127 (2011) 1342-1347.

33 D. Li, X. Liu, L. Lin, J. Hou, N. Li, C. Wang, P. Wang, Q. Zhang, P. Zhang, W. Zhou, Z. Wang, G. Ding, S.M. Zhuang, L. Zheng, W. Tao, X. Cao, MicroRNA-99a inhibits hepatocellular carcinoma growth and correlates with prognosis of patients with hepatocellular carcinoma, J. Biol. Chem. 286 (2011) 36677-36685.

34 G. Caraux, S. Pinloche, PermutMatrix: a graphical environment to arrange gene expression profiles in optimal linear order, Bioinformatics 21 (2005) 1280-1281.

35 H. Yang, W. Gao, L. Liu, K. Liu, E.H. Liu, L.W. Qi, P. Li, Discovery of characteristic chemical markers for classification of aconite herbs by chromatographic profile and probabilistic neural network, J. Pharm. Biomed. Anal. 115 (2015) 10-19.

36 Z.Q. Shi, D.F. Song, R.Q. Li, H. Yang, L.W. Qi, G.Z. Xin, D.Q. Wang, H.P. Song, J. Chen, H. Hao, P. Li, Identification of effective combinatorial markers for quality standardization of herbal medicines, J. Chromatogr. A 1345 (2014) 78-85.

Figure Legends

Fig. 1 The principle (A) and concept (B) of BTPP for characterization of receptor-targeted natural products.

Fig. 2 Screening for a suitable cell for the establishment of BTPP from H9c2 cardiomyocytes (A), human aortal vascular endothelial cells (B) and CHO-M_2 (C).

Fig. 3 Characterization of *Daturae Flos* (A) and the easily confused herbs (B-H) by BTPP.

Fig. 4 Identification of the 7 common components from 20 batches of *DF*.

Fig. 5 (A) The DMR profiling caused by the competition between *DF* and acetylcholine for M_2 receptor. (B) The activity of *DF* exhibits a concentration-dependent manner. The white bar represents the blank control (without acetylcholine), and the black bar represents the acetylcholine group. Data are presented as the mean ± SD (n = 3). $^{\#}p < 0.01$, vs. blank control; $^{*}p < 0.05$, $^{**}p < 0.01$, vs. acetylcholine group.

Fig. 6 Cluster analysis of the Pearson correlation coefficients of 127 peak combinations.

Fig. 7 The quantitative equations, linear ranges, LODs and LOQs of scopolamine (A) and hyoscyamine (B).

Fig. 8 Bioactivity validation of the potential marker compounds in *DF*. The comparison was conducted with the concentration of *DF* as a medium.

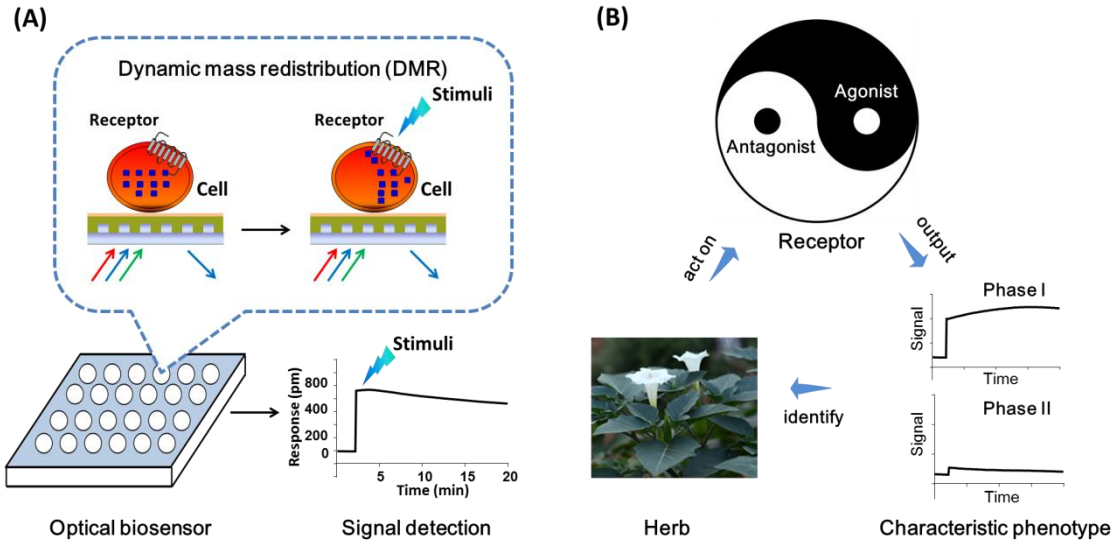

Fig. 1

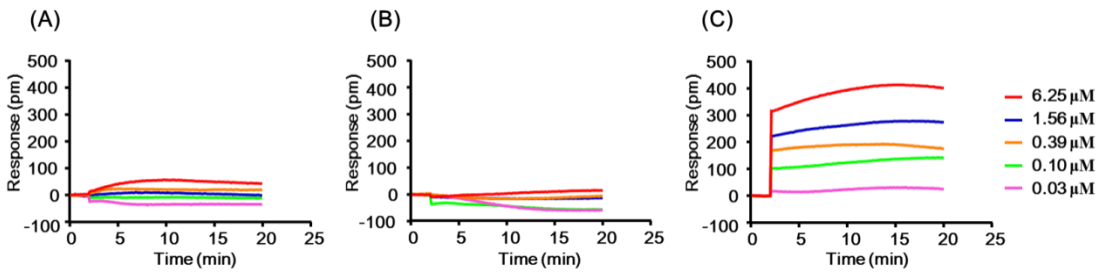

Fig. 2

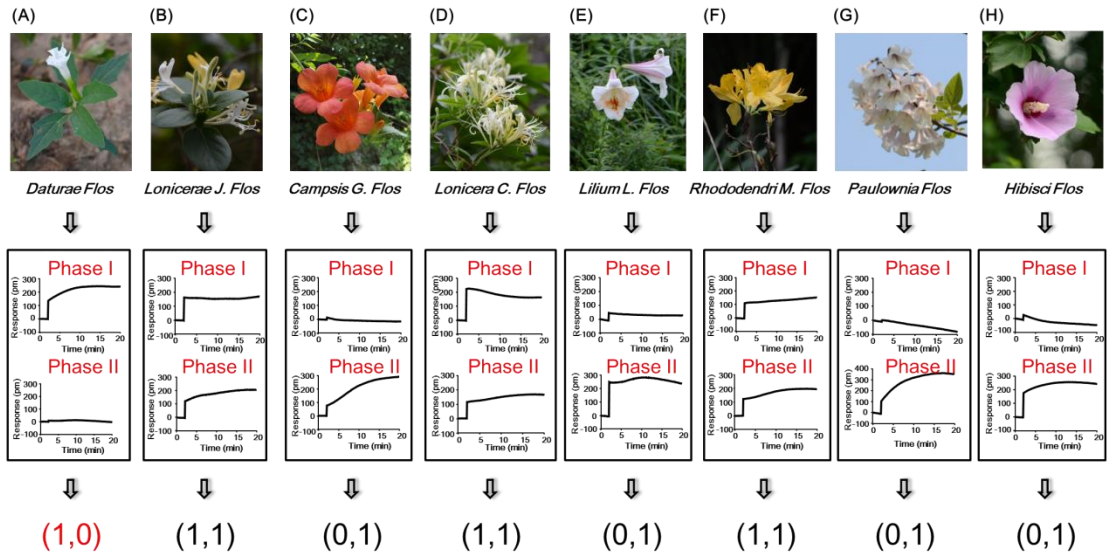

Fig. 3

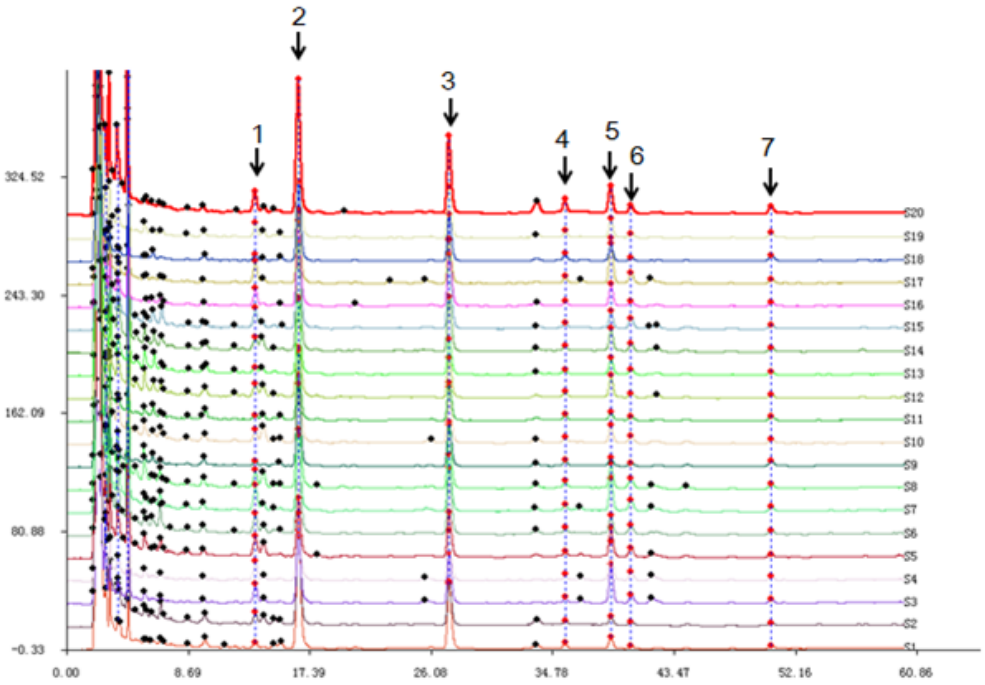

Fig. 4

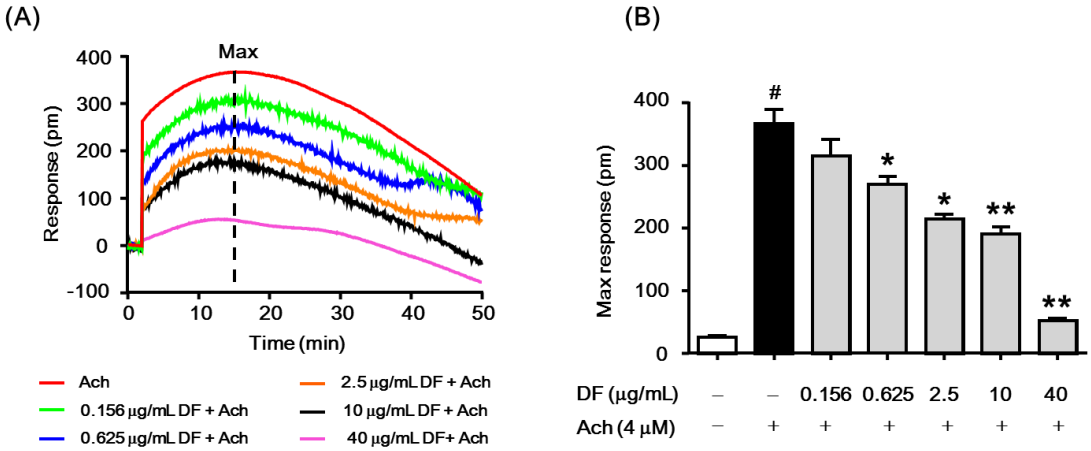

Fig. 5

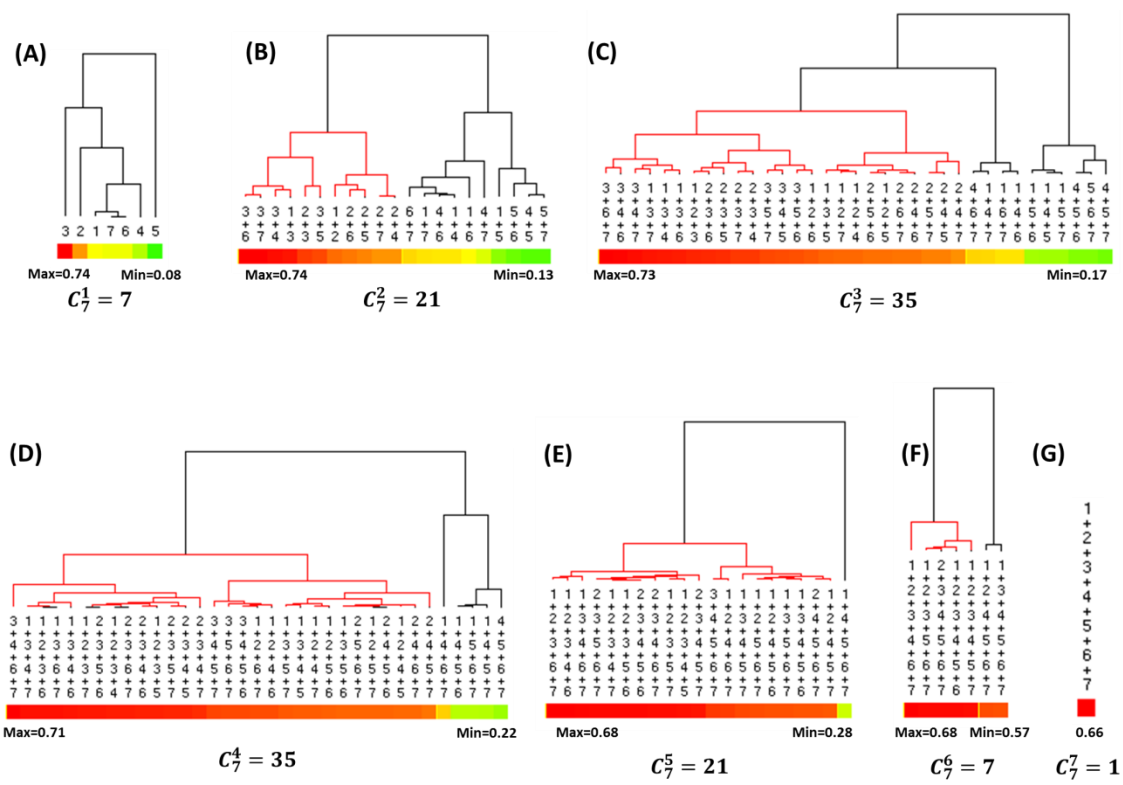

Fig. 6

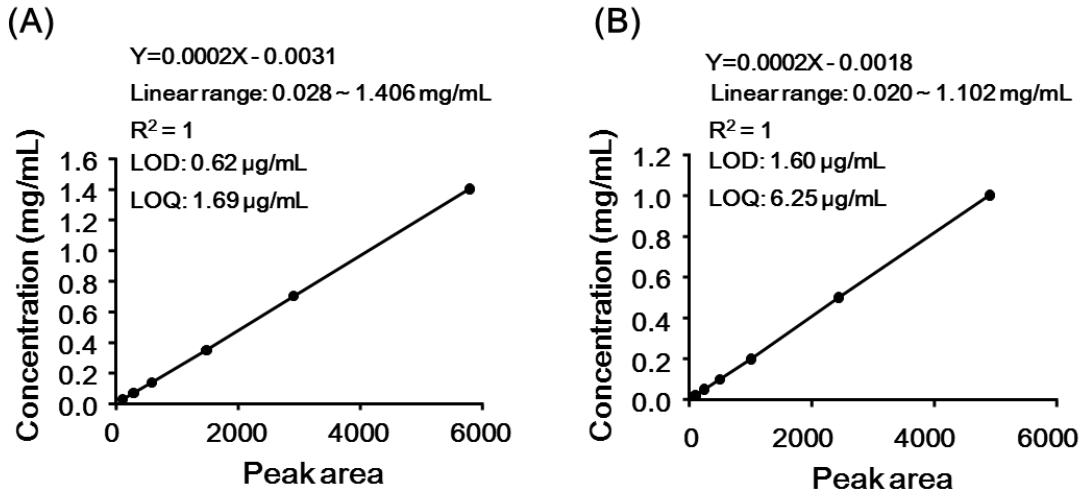

Fig. 7

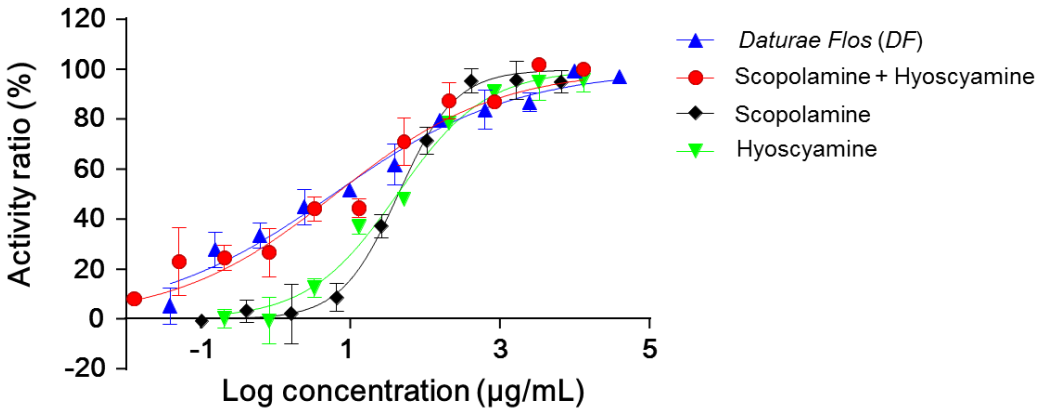

Fig. 8

Table 1 The source, bioactivity and content information (peak 2 and 3) of 20 batches of *Daturae Flos*.

No.	Source	EC_{50} (μg/mL)	95% confidence interval	Peak 2 (mg/mL)	Peak 3 (mg/mL)
1	Guangxi	16.34	11.88-22.47	0.46	0.19
2	Anhui	37.00	33.28-41.14	0.34	0.13
3	Yunnan	21.61	17.04-27.41	0.25	0.15
4	Gansu	35.79	31.95-40.09	0.22	0.13
5	Anhui	5.86	3.63-9.45	0.37	0.22
6	Henan	9.00	5.19-15.60	0.39	0.20
7	Fujian	20.99	15.33-28.73	0.28	0.17
8	Sichuan	9.70	9.53-9.87	0.41	0.19
9	Jiangsu	24.45	19.94-29.97	0.30	0.13
10	Zhejiang	13.00	10.26-16.48	0.35	0.17
11	Guizhou	47.00	42.69-51.75	0.25	0.11
12	Henan	19.16	17.24-21.30	0.36	0.12
13	Guangdong	42.86	31.64-58.05	0.26	0.10
14	Hebei	9.40	8.72-10.14	0.40	0.16
15	Anhui	15.00	10.10-22.28	0.39	0.22
16	Gansu	10.89	5.45-21.77	0.34	0.20
17	Gansu	23.13	16.53-32.36	0.27	0.13
18	Gansu	26.92	25.09-28.88	0.29	0.14
19	Gansu	22.85	21.00-24.85	0.45	0.15
20	Beijing	12.73	8.55-18.97	0.50	0.24

Table 2 Screening for M_2 receptor antagonists from 25 natural compounds by BTPP.

No.	Compound	Phenotypes at different concentrations (μM)		
		100	25	6.25
1	Dauricine	(-1, 1)	(0, 1)	(0, 1)
2	Benzoylhypaconine	(1, 1)	(1, 1)	(1, 1)
3	Benzoylmesaconine	(0, 1)	(0, 1)	(0, 1)
4	Chelerythrine	(1, 0)	(1, 0)	(0, 1)
5	Theophylline	(0, 1)	(0, 1)	(0, 1)
6	Hypaconitine	(0, 1)	(0, 1)	(0, 1)
7	Hordenine	(0, 1)	(0, 1)	(0, 1)
8	Yunaconitine	(1, 1)	(1, 1)	(1, 1)
9	Doxofylline	(0, 1)	(0, 1)	(0, 1)
10	Dihydrocapsaicin	(1, 1)	(1, 1)	(0, 1)
11	Diprophylline	(0, 1)	(0, 1)	(0, 1)
12	Rhynchophylline	(0, 1)	(0, 1)	(0, 1)
13	Homoharringtonine	(0, 1)	(0, 1)	(0, 1)
14	Trigonelline	(0, 1)	(0, 1)	(0, 1)
15	Cyclovirobuxine	(1, 1)	(1, 1)	(1, 1)
16	Sanguinarine	(-1, 0)	(-1, 0)	(-1, 0)
17	Jatrorrhizine Hydrochloride	(-1, 1)	(-1, 1)	(0, 1)
18	Palmatine hydrochloride	(0, 1)	(0, 1)	(0, 1)
19	Ephedrine hydrochloride	(0, 1)	(0, 1)	(0, 1)
20	Papaverine hydrochloride	(-1, 1)	(-1, 1)	(-1, 1)
21	Protopine	(0, 1)	(0, 1)	(0, 1)
22	Berberine hydrochloride	(0, 1)	(0, 1)	(0, 1)
23	(+)-Corynoline	(-1, 1)	(-1, 1)	(0, 1)
24	10-hydroxycamptothecin	(0, 1)	(0, 1)	(0, 1)
25	7-Ethyl-10-hydroxycamptothecin	(0, 1)	(0, 1)	(0, 1)

Table 3 The potential mechanism comparison of chelerythrine, sanguinarine, scopolamine and hyoscyamine by molecular docking and pharmacophore modeling.

Compound	EC_{50} (μM)	Structure	Pharmacophore	Docking
Scopolamine	0.27	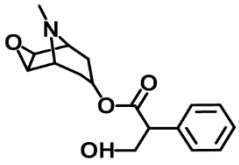	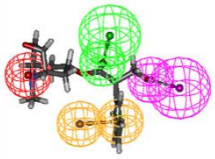	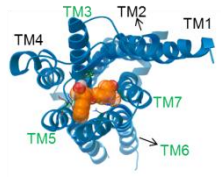
Hyoscyamine	0.16	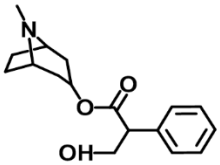	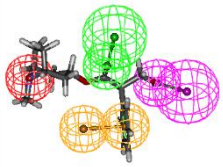	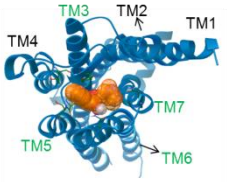
Chelerythrine	14.29	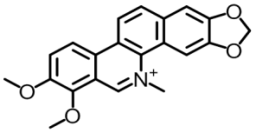		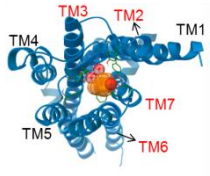
Sanguinarine	5.65